Earth and Planetary Science Letters 509 (2019) 9–14

Contents lists available at ScienceDirect

Earth and Planetary Science Letters

www.elsevier.com/locate/epsl

Large scale lithospheric detachment of the downgoing Cocos plate: The 8 September 2017 earthquake (M_w 8.2)

Gerardo Suárez *, Miguel A. Santoyo, Vala Hjorleifsdottir, Arturo Iglesias, Carlos Villafuerte, Victor M. Cruz-Atienza

Instituto de Geofísica, Universidad Nacional Autónoma de México, Mexico

ARTICLE INFO

Article history:
Received 16 July 2018
Received in revised form 28 November 2018
Accepted 19 December 2018
Available online xxxx
Editor: J.P. Avouac

Keywords:
Middle American Trench
Tehuantepec
8 September 2017 earthquake
lithospheric detachment
intraslab earthquake

ABSTRACT

On 8 September 2017, a great earthquake (M_w 8.2) took place in the Mexican subduction zone in the Tehuantepec gap, where no large subduction earthquakes have taken place since 1902. However, the 8 September earthquake did not occur on the contact between the Cocos and North American plates. The centroidal hypocentral depths reported by different agencies, including the National Seismological Service, range from 45 to 47.4 km, placing it immediately beneath the down-dip limit of the interplate locked zone. The source mechanism reflects down-dip tensional faulting. The inversion of the fault process shows a rupture that initiated at the bottom of the lithosphere and propagated upward, breaking through the entire subducted lithosphere. An unusually long, complex and copious aftershock sequence followed the main event. The relocated aftershocks, in the first 20 days following the main event, delineate a 160-km-long fault, sub-parallel to the oceanic trench, immediately beneath the interplate contact. The aftershocks also concentrate in secondary intraslab faults ~50 km down-dip from the mainshock rupture, revealing that pervasive tensional stresses are present within the subducted plate. This deformation pattern suggests a large-scale tensional regime in the slab, apparently induced by its own gravitational weight that pulls it away from the strongly coupled interplate contact. Other large intraplate earthquakes in the vicinity, in 1931 (M_w 7.8) and 1999 (M_w 7.5), also reflect this detachment of the downgoing Cocos plate that sinks into the mantle under its own gravitational weight. The slab detachment suggests that the up-dip segment of the plate interface near the Isthmus of Tehuantepec is locked and possibly primed for a megathrust earthquake, such as the M_w 8.6 that took place in 1787, on an adjacent segment of the Mexican subduction zone.

1. Tectonic setting of the Tehuantepec subduction zone

The Gulf of Tehuantepec shows drastic differences in geometry and in seismic behaviour from the rest of the Mexican subduction zone. One of the more salient features in this region is the subduction of the bathymetric feature known as the Tehuantepec Ridge (TR). The TR is a long and linear bathymetric high that separates the Cocos plate into two zones of different age and tectonic characteristics (Manea et al., 2005). At its intersection near the Middle American Trench (MAT), the highly asymmetric TR rises 400 to 1,100 m above the average ocean floor depth (Manea et al., 2005). Although the reasons are not understood, the TR marks also the border where the subducted Cocos plate changes dip from sub horizontal subduction beneath Central Mexico to one dipping at ~45° beneath south-eastern Mexico and Central America (Pardo and Suárez, 1995; Bravo et al., 2004; Ponce et al., 1992).

Where the TR subducts beneath the North American plate, it sharply deflects the trench and the coastline inland (Fig. 1). The Tehuantepec segment of the MAT is identified as a seismic gap where no large earthquakes are known to have occurred on the plate contact at least since 1902 (Fig. 1) (Kelleher et al., 1973; Kelleher and McCann, 1976; Nishenko, 1991). The crustal earthquakes of moderate magnitude in the northern part of the Isthmus of Tehuantepec have been attributed to the deformation of the overriding plate in response to the compressive stress induced by the subduction of this bathymetric high (Suárez and López, 2015). It is in this complex tectonic setting that the great 2017 Tehuantepec earthquake took place.

* Correspondence to: Instituto de Geofísica, UNAM, Ciudad Universitaria, CDMX 14010, Mexico.
E-mail address: gerardo@geofisica.unam.mx (G. Suárez).

https://doi.org/10.1016/j.epsl.2018.12.018
0012-821X/

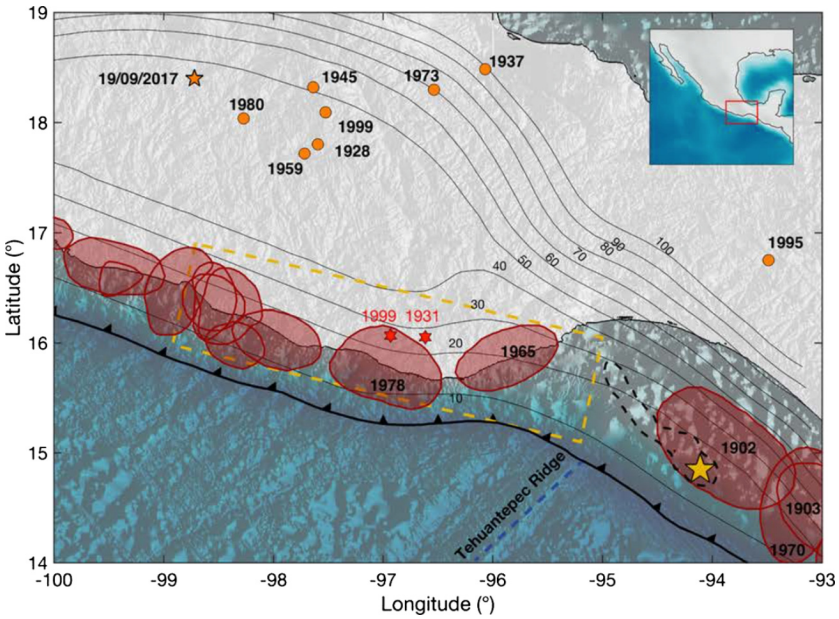

Fig. 1. Major tectonic features of the subduction zone in the Isthmus of Tehuantepec. The red ovals indicate the rupture areas of the more important subduction earthquakes. Red stars indicate the location of the 1931 and 1999 normal faulting earthquakes; gold star the 8 September 2017 and orange star the 19 September 2017 event. The dotted yellow line shows the rupture zone of the 1787 earthquake (Suárez and Albini, 2009). Contours indicate the dip of the subducted slab beneath the North American plate (Pardo and Suárez, 1995) and red dots are in-slab earthquakes in the subducted Cocos plate.

2. Inversion of the kinematic behaviour of the fault rupture

The kinematic rupture history of the Tehuantepec earthquake was studied using body and surface waves recorded by the global seismic networks, using a simulated annealing, wavelet method (Ji et al., 2002a, 2002b; Shao et al., 2011), which minimizes the weighted difference between wavelet coefficients of observed and synthetic seismograms. In order to determine the temporal and spatial distribution of slip on the fault plane, the far-field seismograms were deconvolved to obtain displacement.

We used records of stations located at distances from 30° to 90°. The observed seismograms were filtered and windowed into two data sets: 1) The body-waves were band-pass filtered between 1 and 100 s; 2) surface waves, were band-pass filtered between 170 and 250 s, in a time window between 0 and 3600 s. The inversion is performed using the Fast Finite Fault (FFF) inversion algorithm (Ji et al., 2002a; Shao et al., 2011). The slip on each fault has an asymmetric time function and smoothing is applied both to the slip distribution and to the rupture contours (Shao et al., 2011).

The results of the inversion show an inhomogeneous slip distribution on the near vertical fault (dip = 81°) on which the Tehuantepec earthquake occurred. The rupture initiated at a depth of ∼57 km and the fault rupture propagated updip and to the northwest on a fault with a strike of 315°. Near the hypocentre, both the slip and the areal extent of the rupture are relatively small, reaching a maximum slip of ∼3 m (Fig. 2). The main rupture took place in the upper part of the Cocos lithosphere, at depths of 25 to 45 km. Here, the maximum slip reaches ∼15 m.

The large slip in the upper part of the slab induced deformation also in the overriding plate. Interferometry data suggest subsidence of up to 20 cm of the coast near the northwestern end of the rupture zone (NASA, 2017). This coastal deformation generated a tsunami observed along the Tehuantepec coast with a maximum runup height of 3 m (Ramírez-Herrera et al., 2018).

Compared to scaling laws of shallow depth, normal faulting earthquakes, the slip is much larger than expected (Wells and Coppersmith, 1994; Wesnousky, 2008). Also, the empirical relations between source dimensions of intraslab events and moment magnitude (Strasser et al., 2010) suggest that the rupture area for an earthquake of this magnitude should be about four times larger than the fault area where the main slip occurred. Thus the rupture of the 2017 earthquake is very energetic, in agreement with observations that intraslab earthquakes tend to radiate more energy than interplate events (Ye et al., 2017).

3. Relocation of aftershocks and the complex stress distribution in the slab

The Tehuantepec earthquake was followed by an unusually long and active aftershock sequence. A worldwide comparative analysis of aftershocks showed that the MAT has a relatively small number of aftershocks after large subduction earthquakes (Singh and Suárez, 1988). In contrast, over 30,000 aftershocks have been recorded in the twelve months following the 2017 Tehuantepec earthquake. Admittedly, the analysis of aftershocks of large subduction earthquakes in the MAT (Singh and Suárez, 1988) should not be compared directly with this intraplate earthquake. Nevertheless, the number of aftershocks after the Tehuantepec earthquake is unusually copious and complex. Also, the majority of the aftershocks were located outside the main rupture area, as we show below.

Most of the aftershocks were smaller than magnitude 5.5. The epicentral locations of these earthquakes and, in particular, the hypocentral depths reported by the Seismological Service of Mexico (SSN), are very poorly controlled due to the location of the aftershock sequence offshore and the dearth of seismic stations in the Isthmus of Tehuantepec (Fig. 3). We relocated the aftershocks reported by the SSN within the first 20 days after the main event using the double difference algorithm (Waldhauser and Ellsworth, 2000). The relocations were calculated using a flat-layered *S*-wave velocity model obtained from the analysis of the group velocity of Rayleigh wave dispersion curves, using a multiple filter technique. The flat-layered, *S*-wave velocity model used to relocate the aftershocks was inverted from the dispersion curves using a simulated annealing scheme (Dziewonski et al., 1969; Berteussen, 1977; Iglesias et al., 2001).

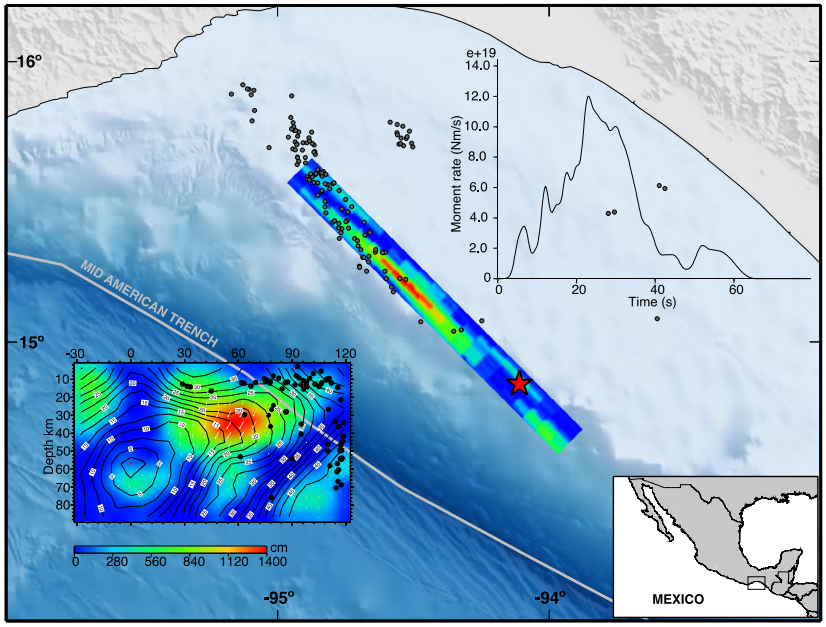

Fig. 2. Results of the kinematic inversion of the rupture process of the 2017 Tehuantepec earthquake. The colour swath on the map is the fault extent in plan view. The inset in the lower left shows the slip distribution on the fault; black dots are the relocated hypocentres in the first 48 h after the main event. The source time function is shown in the upper right corner.

The arrival times of *P*- and *S*-waves reported by the Mexican Seismological Service were used in the algorithm, which makes use of the residuals between observed and theoretical travel-time differences and minimizes this observation for pairs of earthquakes at each station. The least-squares solution is found by iteratively adjusting the differences between hypocentral pairs. In the analysis we eliminated the aftershocks that took place after the 23 September 2017 earthquake. This is a crustal earthquake at a depth of 10 km. Although it is probably related to the shallow deformation of the North American plate due to the rupture of the 8 September earthquake, it is not part of the seismicity occurring within the subducted slab. Being a crustal earthquake, outside of the main rupture, it is the subject of a separate study.

A total of 305 aftershocks were relocated. Their distribution shows a complex spatial pattern. Although some aftershocks clearly map the 150-km long fault that ruptured during the great September earthquake, the majority of the events lie outside of the main fault (Fig. 3). The rupture area of the mainshock is clearly delineated by aftershocks occurring on a fault plane oriented northwest southeast, which extend from depths of approximately 20 to 60 km (Figs. 2–4). The hypocentre of the main shock lies at the bottom of the almost vertical aftershock alignment. This is in agreement with the fault plane determined in the finite fault model and the focal mechanism of the Tehuantepec earthquake (Sections BB′ and CC′, Fig. 4).

The majority of the earthquakes on the main rupture occurred within the first week after the mainshock (Fig. 3). Both the aftershock distribution and the finite fault model strongly suggest that the fault broke the entire Cocos plate lithosphere. The thickness of the slab is estimated to be approximately 35 km, assuming the transition temperature at the bottom of the lithosphere is ∼1300° (Fig. 3) (Caldwell and Turcotte, 1979; Manea and Manea, 2006).

Besides the number of aftershocks and its unusually long duration, an unusual observation in the case of the Tehuantepec earthquake is that most of the aftershocks are located off the main rupture in five separate clusters within the slab (Fig. 3). Three of these clusters (Sections AA′, BB′, and CC′, Fig. 4) are located 30 km down-dip of the mainshock within the subducted slab. They reveal secondary faulting within the subducted Cocos plate, on parallel

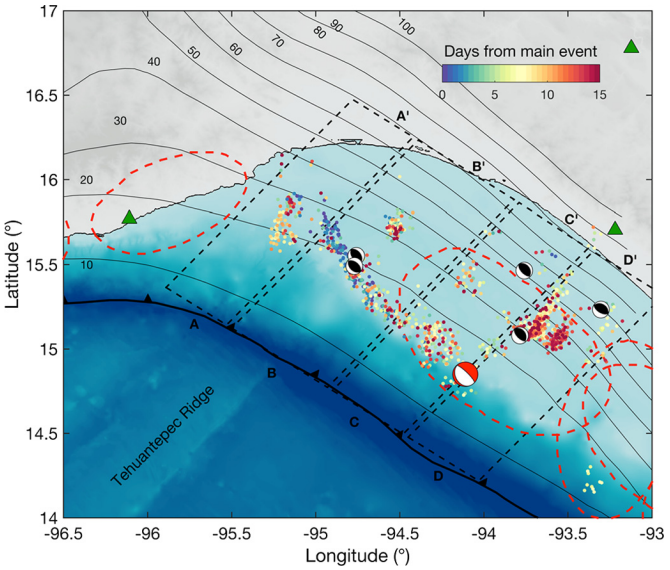

Fig. 3. Relocated aftershocks during the first 20 days after the 2017 Tehuantepec earthquake are shown as a function of their time of occurrence (see colour code). Focal mechanisms of the main shock (red symbol) and of the aftershocks (black symbols) are shown on a lower hemispheric projection where the dark quadrants indicate compressional first motions. The boxes labelled AA′, BB′, CC′ and DD′ indicate in plan view the cross sections on Fig. 4. The green triangles are the seismological stations of the Seismological Service of Mexico. Slab contours as on Fig. 1.

faults located 30 km down-dip of the main 8 September rupture. These aftershock sequences suggest faults that extend also through the whole oceanic lithosphere. Although these aftershocks do not define a single and continuous fault parallel to the main rupture, they suggest the activation of individual faults within the slab, down-dip of the main fault where the Tehuantepec earthquake occurred. Unfortunately, there are no unambiguous focal mechanisms of aftershocks in these clusters.

Another group of aftershocks is located to the northeast of the M_w 8.2 epicentre (Section DD′, Fig. 4). This earthquake sequence became active approximately one week after the mainshock and

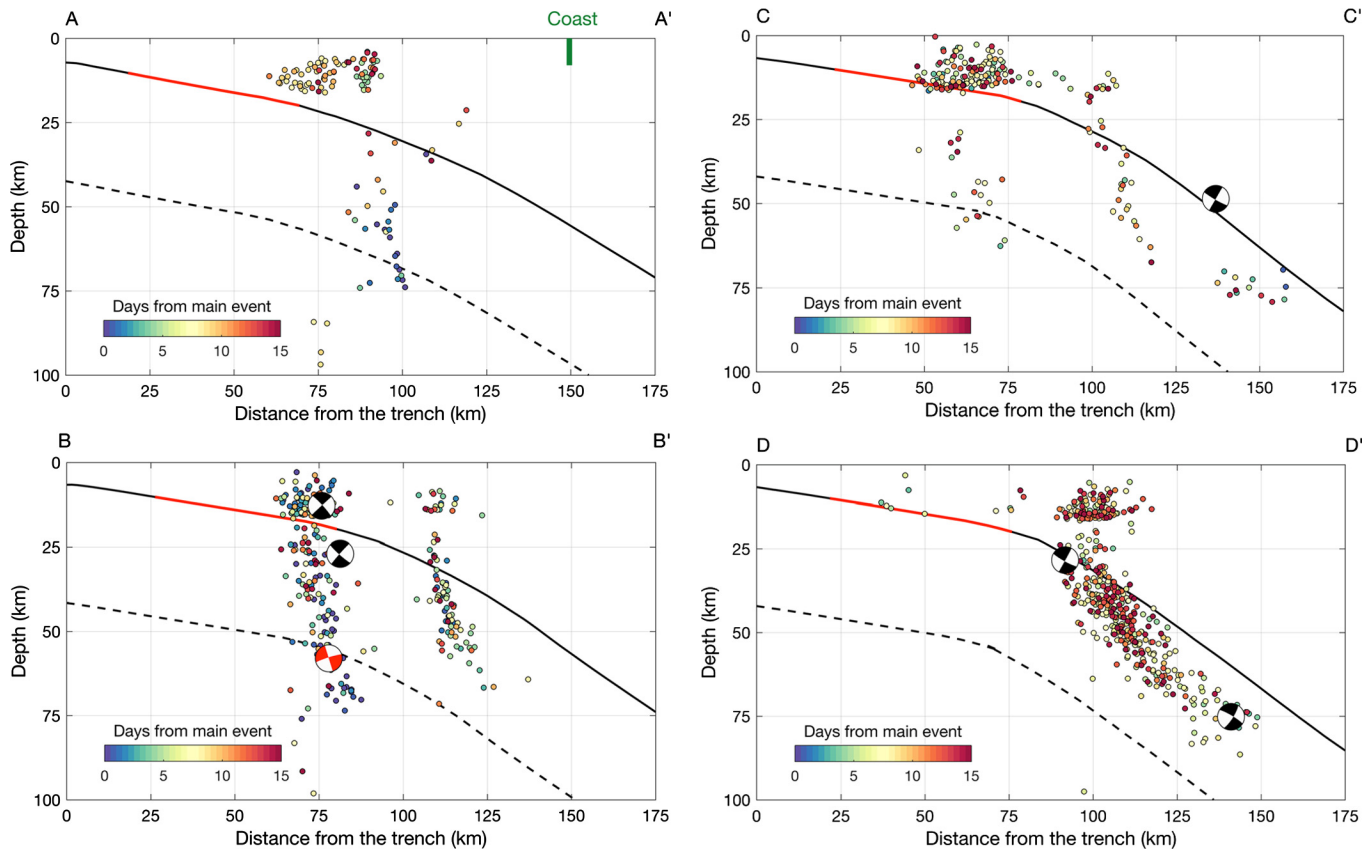

Fig. 4. Cross-sections AA′, BB′, CC′ and DD′ (Fig. 3). The colour code of the hypocentres shows the time of occurrence of the aftershocks after the main event. The source mechanism of the 2017 Tehuantepec earthquake (red) and of the relocated aftershocks (black) is shown on side-looking lower hemispheric projections, where the dark quadrants are compressional first motions. The cross-sections are drawn based on the dip of the slab (Pardo and Suárez, 1995; Bravo et al., 2004; Ponce et al., 1992). The thickness of the downgoing plate is estimated assuming a 1300° isotherm at the bottom of the elastic lithosphere (Caldwell and Turcotte, 1979; Manea and Manea, 2006). The down dip extent of the megathrust plate contact is shown as a red line and assumed to have a maximum depth of 20 km, as observed for the 19 September 1985 earthquake (M_w 8.1) (Suárez and Sánchez, 1996; UNAM Seismology Group, 1986) and for other large earthquakes in the Mexican subduction zone (UNAM Seismology Group, 2015).

ranges in depth from 25 to 85 km. These aftershocks follow the dip of the subducted Cocos plate (Pardo and Suárez, 1995; Bravo et al., 2004; Ponce et al., 1992).

For the larger aftershocks ($M_w \geq 4.3$) reported by the Seismological Service of Mexico (SSN), moment tensors were determined using a regional moment tensor inversion (Pasyanos et al., 1996). The Green functions were calculated with a spacing of 5 km on the horizontal and vertical directions. The algorithm searches the data in combinations of three seismic stations based on distance criteria determined by the magnitude of the earthquake. Each inversion is weighted by a function that is inversely proportional to the azimuthal gap of the recording stations. Thus the station combination with the smallest gap is given preference. For each station combination, a grid search is conducted using a spacing average of ±30 km. A quality estimation of the moment tensor inversions is based on the inverse function of the azimuthal gap and the variance reduction resulting from the inversion. Here we use only moment tensors showing a 60% reduction in variance.

Due to the poor azimuthal coverage of local seismic stations, only two earthquakes in this cluster of aftershocks (Section DD′, Fig. 4) attain the prescribed variance reduction of 60%. These mechanisms show that the T-axes of both events are aligned with the dip of the slab, suggesting the pervasive down-dip tensional deformation of the subducted Cocos plate.

Some aftershocks are apparently located in the upper plate at depths of ∼12 km. These aftershocks began about one week after the mainshock. Unfortunately, it is unclear whether these events occurred within the subducted Cocos plate or whether they reflect deformation of the upper North American plate. We were unable to determine reliable source mechanisms for these clusters of aftershocks.

The shallow aftershocks (Sections BB′ and CC′ on Fig. 4) are located above the main rupture, suggesting they may be interplate earthquakes on the downdip end of the megathrust plate contact. In the Mexican subduction zone, the maximum depth of the seismogenic plate contact is shallow and does not extend below 20 km (Suárez and Sánchez, 1996; UNAM Seismology Group, 1986; UNAM Seismology Group, 2015). The focal mechanisms determined for two events indicate thrust faulting, probably related to the relative motion of the Cocos plate beneath North America.

4. Coulomb failure stress changes induced by the Tehuantepec earthquake

We computed the static stress field change associated with our finite source solution (Nikkhoo and Walter, 2015) and calculated the Coulomb Failure stress change (ΔCFS) induced by the main event on thrust-like faults on the plate interface considering a 3D local geometry of the region (Pardo and Suárez, 1995; Bravo et al., 2004; Ponce et al., 1992) following:

$$\Delta CFS = \Delta\tau + \mu' \Delta\sigma_n$$

where, $\Delta\tau$ represents the change of the shear stress in the direction of the fault slip, $\Delta\sigma_n$ is the change of the fault normal stress (positive for tension), and μ' is the apparent coefficient of friction assumed to be 0.4.

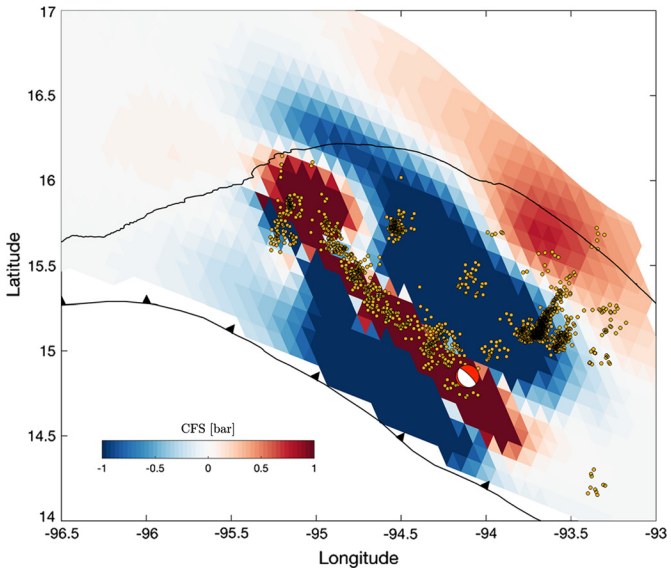

Fig. 5. Changes in the Coulomb Failure stress induced by the M_w 8.2 Tehuantepec earthquake on the plate interface. The red and blue colours represent the regions where failure is enhanced and inhibited, respectively. The yellow circles are the relocated aftershocks described in the text. The focal mechanism of the main event is represented by a lower-hemispheric projection where the red areas indicate compressional first motions.

The Coulomb stress change analysis (Nikkhoo and Walter, 2015) suggests that most of the aftershocks fall where the main rupture induced positive Coulomb failure stresses (Fig. 5). Thus these earthquakes may be shallow-thrust events on the seismogenic plate interface, apparently induced by the slip on the main fault (Sections BB′ and CC′, Fig. 4).

5. Implications of the 2017 Tehuantepec earthquake

As mentioned, this segment of the Mexican subduction zone is a seismic gap where no great earthquakes are reported in the instrumental and historical catalogues. The last great earthquake occurred in 1902 and its location is very uncertain (Kelleher et al., 1973; Kelleher and McCann, 1976; Nishenko, 1991). The Tehuantepec ridge offshore the subduction zone is a bathymetric high that appears to be deforming and deflecting the trench and the overriding plate (Figs. 1), suggesting strong coupling on the plate interface. Additional evidence comes from the regional slip deficit observed in the Tehuantepec region from geodetic studies (Franco et al., 2012; Nikkhoo and Walter, 2015). The absence of great earthquakes and the buoyant nature of the Tehuantepec ridge indicate that this segment of the Mexican subduction zone is a mature seismic gap where seismic energy is accumulating.

The 8 September 2017 earthquake broke through the entire subducting lithosphere suggesting that: (1) the seismogenic zone of the plate interface in the Gulf of Tehuantepec is strongly locked and (2) the slab is being detached by its own gravitational weight. The large-scale tensional deformation within the subducted Cocos plate, revealed by this unusual aftershock sequence, emphasizes that the subducting slab is under extensive tensional down-dip stress. This suggests that the seismogenic zone on the plate interface is highly coupled, preventing the slab penetration into the asthenosphere. As a result, the subducting slab undergoes massive extensional detachment due to its gravitational pull.

Stress transfer in strongly coupled subduction zones is interpreted as the reason for large earthquakes to occur down-dip of the coupled interface segment (Astiz et al., 1988; Christensen and Ruff, 1988; Lay et al., 1989; Mikumo et al., 2002). The 1977 Tonga earthquake (M_w 8.1) is a similar example of an intraplate event occurring down-dip of a strongly coupled subduction zone, where the Louisville ridge subducts (Christensen and Ruff, 1988). It is worth noting that in this part of the Mexican subduction zone, two other large, normal-faulting earthquakes took place with similar tectonic characteristics, immediately beneath the seismogenic plate contact: the 15 January 1931 Oaxaca (M_w 7.8) and the 30 September 1999 (M_w 7.5) (Singh et al., 1985, 2000). Other authors have suggested bending stresses in the downgoing slab as the cause for the large Tehuantepec earthquake (Okuwaki and Yagi, 2017; Chen et al., 2018).

Large intraplate earthquakes in the subducted slab are relatively uncommon in subduction zones. We speculate that the high tensional stresses suggested by the presence of these great earthquakes that break the shallow part of the slab, reflect a strongly coupled plate contact in the Gulf of Tehuantepec. The locked plate interface would transfer the stress to the subducted slab. A megathrust earthquake ($M_w \sim 8.6$) took place in this same area in 1787, producing the largest tsunami recorded in the Central American subduction zone (Suárez and Albini, 2009). This earthquake was much larger than the average M_w 7.9 to 8.1 thrust events recorded by the instrumental seismic catalogue during the last 120 years. The length of the MAT segment encompassing these tensional, intraplate events in the Cocos slab is similar to that estimated for the 1787 earthquake (Fig. 1), leaving open the possibility that a similar event could occur in this region with potentially devastating consequences.

Declaration on competing or conflict of interest

The authors have no competing or conflict of interest in what is expressed in this manuscript.

Author contributions

G.S. coordinated the work of the team, wrote the initial draft of the paper, collaborated in the aftershock relocations and was in charge of the final edition.

M.A.S. was responsible for the relocation of the aftershock sequence using the data from the Mexican Seismological Service (SSN).

V.H. inverted the kinematic source function of the main earthquake.

A.I. determined the seismic velocity model used in the relocation process and obtained the moment tensor inversions.

C.V. Estimated the Coulomb stress transfer of the fault and drafted most of the figures.

V.M.C.A. Participated in the estimation of the Coulomb stress transfer, and collaborated in the location of the aftershocks and in drafting of the paper.

Acknowledgements

We thank X. Pérez-Campos and V.H. Espíndola, from the Mexican Seismological Service (*SSN*), for the data used in the relocation analysis. The data used for the kinematic inversion of the fault are from the Data Management Center (*DMC*) of the Incorporated Research Institutions for Seismology (*IRIS*). We thank our colleagues in the Department of Seismology of the Instituto de Geofísica, UNAM for helpful discussions and two anonymous reviewers for helpful corrections and suggestions. Research funded by a grant from the Mexican National Council for Science and Technology (CONACYT) number PN2015-639.

References

Astiz, L., Lay, T., Kanamori, H., 1988. Large intermediate-depth earthquakes and the subduction process. Phys. Earth Planet. Inter. 53 (1–2), 80–166.

Berteussen, K.A., 1977. Moho depth determinations based on spectral-ratio analysis of NORSAR long-period P waves. Phys. Earth Planet. Inter. 15 (1), 13–27.
Bravo, H., Rebollar, C., Uribe, A., Jimenez, O., 2004. Geometry and state of stress of the Wadati–Benioff zone in the Gulf of Tehuantepec, Mexico. J. Geophys. Res. 109. https://doi.org/10.1029/2003JB002854.
Caldwell, J.G., Turcotte, D.L., 1979. Dependence of the thickness of the elastic oceanic lithosphere on age. J. Geophys. Res., Solid Earth 84 (B13), 7572–7576.
Chen, K., Feng, W., Liu, Z., Tony Song, Y., 2018. 2017 M w 8.1 Tehuantepec earthquake: deep slip and rupture directivity enhance ground shaking but weaken the Tsunami. Seismol. Res. Lett. 89 (4), 1314–1322. https://doi.org/10.1785/0220170277.
Christensen, D.H., Ruff, L.J., 1988. Seismic coupling and outer rise earthquakes. J. Geophys. Res., Solid Earth 93 (B11), 13421–13444.
Dziewonski, A., Bloch, S., Landisman, M., 1969. A technique for the analysis of transient seismic signals. Bull. Seismol. Soc. Am. 59 (1), 427–444.
Franco, A., Lasserre, C., Lyon-Caen, H., Kostoglodov, V., Molina, E., Guzman-Speziale, M., Barrier, E., 2012. Fault kinematics in northern Central America and coupling along the subduction interface of the Cocos Plate, from GPS data in Chiapas (Mexico), Guatemala and El Salvador. Geophys. J. Int. 189 (3), 1223–1236.
Iglesias, A., Atienza, V.C., Shapiro, N.M., Singh, S.K., Pacheco, J.F., 2001. Crustal structure of south-central Mexico estimated from the inversion of surface-wave dispersion curves using genetic and simulated annealing algorithms. Geofís. Int. 40 (3), 181–190.
Ji, C., Wald, D.J., Helmberger, D.V., 2002a. Source description of the 1999 Hector Mine, California, earthquake, part I: wavelet domain inversion theory and resolution analysis. Bull. Seismol. Soc. Am. 92, 1192–1207.
Ji, C., Wald, D.J., Helmberger, D.V., 2002b. Source description of the 1999 Hector Mine, California, earthquake, part II: complexity of slip history. Bull. Seismol. Soc. Am. 92 (4), 1208–1226.
Kelleher, J., McCann, W., 1976. Buoyant zones, great earthquakes, and unstable boundaries of subduction. J. Geophys. Res. 81 (26), 4885–4896.
Kelleher, J.A., Sykes, L.R., Oliver, J., 1973. Possible criteria for predicting earthquake locations and their application to major plate boundaries of the Pacific and the Caribbean. J. Geophys. Res. 78, 2547–2585.
Lay, T., Astiz, L., Kanamori, H., Christensen, D.H., 1989. Temporal variation of large intraplate earthquakes in coupled subduction zones. Phys. Earth Planet. Inter. 54 (3–4), 258–312.
Manea, V.C., Manea, M., 2006. Origin of the modern Chiapanecan volcanic arc in southern Mexico inferred from thermal models. In: Volcanic Hazards in Central America. In: Geological Society of America Special Papers, vol. 412, pp. 27–38.
Manea, M., Manea, V.C., Ferrari, L., Kostoglodov, V., Bandy, W.L., 2005. Tectonic evolution of the Tehuantepec Ridge. Earth Planet. Sci. Lett. 238 (1–2), 64–77.
Mikumo, T., Yagi, Y., Singh, S.K., Santoyo, M.A., 2002. Coseismic and postseismic stress changes in a subducting plate: possible stress interactions between large interplate thrust and intraplate normal-faulting earthquakes. J. Geophys. Res., Solid Earth 107 (B1).
National Aeronautics and Space Administration (NASA), Jet Propulsion Laboratory (JPL), California Institute of Technology (CALTECH), Advanced Rapid Imaging and Analysis Team, 2017. 2017 09 08 Chiapas Mexico earthquake. https://aria.jpl.nasa.gov/node/65.
Nikkhoo, M., Walter, T.R., 2015. Triangular dislocation: an analytical, artefact-free solution. Geophys. J. Int. 201 (2), 1119–1141.
Nishenko, S.P., 1991. Circum-pacific seismic potential: 1989–1999. Pure Appl. Geophys. 135, 169–259.
Okuwaki, R., Yagi, Y., 2017. Rupture process during the Mw 8.1 2017 Chiapas Mexico earthquake: shallow intraplate normal faulting by slab bending. Geophys. Res. Lett. 44, 11,816–11,823. https://doi.org/10.1002/2017GL075956.
Pardo, M., Suárez, G., 1995. Shape of the subducted Rivera and Cocos plates in southern Mexico: seismic and tectonic implications. J. Geophys. Res., Solid Earth 100 (B7), 12357–12373.
Pasyanos, M.E., Dreger, D.S., Romanowicz, B., 1996. Towards real-time determination of regional moment tensors. Bull. Seismol. Soc. Am. 86, 1255–1269.
Ponce, L., Gaulon, R., Suárez, G., Lomas, E., 1992. Geometry and state of stress of the downgoing Cocos plate in the Isthmus of Tehuantepec, Mexico. Geophys. Res. Lett. 19 (8), 773–776.
Ramírez-Herrera, M.T., Corona, N., Ruiz-Angulo, A., Melgar, D., Zavala-Hidalgo, J., 2018. The 8 September 2017 tsunami triggered by the M w 8.2 intraplate earthquake, Chiapas, Mexico. Pure Appl. Geophys. 175 (1), 25–34.
Shao, G., Li, X., Ji, C., Maeda, T., 2011. Focal mechanism and slip history of the 2011 M w 9.1 off the Pacific coast of Tohoku Earthquake, constrained with teleseismic body and surface waves. Earth Planets Space 63 (7), 9.
Singh, S.K., Suárez, G., 1988. Regional variation in the number of aftershocks (mb $\geqq$ 5) of large, subduction-zone earthquakes (Mw $\geqq$ 7.0). Bull. Seismol. Soc. Am. 78 (1), 230–242.
Singh, S.K., Suárez, G., Domínguez, T., 1985. The Oaxaca, Mexico, earthquake of 1931: lithospheric normal faulting in the subducted Cocos plate. Nature 317, 56–58. https://doi.org/10.1038/317056a0.
Singh, S.K., et al., 2000. The Oaxaca earthquake of 30 September 1999 (Mw = 7.5): a normal-faulting event in the subducted Cocos Plate. Seismol. Res. Lett. 71, 67–78. https://doi.org/10.1785/gssrl.71.1.67.
Strasser, F.O., Arango, M.C., Bommer, J.J., 2010. Scaling of the source dimensions of interface and intraslab subduction-zone earthquakes with moment magnitude. Seismol. Res. Lett. 81 (6), 941–950.
Suárez, G., Albini, P., 2009. Evidence for great tsunamigenic earthquakes (M 8.6) along the Mexican subduction zone. Bull. Seismol. Soc. Am. 99 (2A), 892–896.
Suárez, G., López, A., 2015. Seismicity in the southwestern Gulf of Mexico: evidence of active back arc deformation. Rev. Mex. Cienc. Geol. 32 (1).
Suárez, G., Sánchez, O., 1996. Shallow depth of seismogenic coupling in southern Mexico: implications for the maximum size of earthquakes in the subduction zone. Phys. Earth Planet. Inter. 93 (1–2), 53–61.
UNAM Seismology Group, 1986. The September 1985 Michoacan earthquakes: aftershock distribution and history of rupture. Geophys. Res. Lett. 13 (6), 573–576.
UNAM Seismology Group, 2015. Papanoa, Mexico earthquake of 18 April 2014 (Mw 7.3). Geofís. Int. 54 (4).
Waldhauser, F., Ellsworth, W.L., 2000. A double-difference earthquake location algorithm: method and application to the northern Hayward fault, California. Bull. Seismol. Soc. Am. 90 (6), 1353–1368.
Wells, D.L., Coppersmith, K.J., 1994. New empirical relationships among magnitude, rupture length, rupture width, rupture area, and surface displacement. Bull. Seismol. Soc. Am. 84 (4), 974–1002.
Wesnousky, S.G., 2008. Displacement and geometrical characteristics of earthquake surface ruptures: issues and implications for seismic-hazard analysis and the process of earthquake rupture. Bull. Seismol. Soc. Am. 98 (4), 1609–1632.
Ye, L., Lay, T., Kanamori, H., Rivera, L.J., 2017. The 2017 Mw 8.2 Chiapas, Mexico earthquake: energetic slab detachment. Geophys. Res. Lett. https://doi.org/10.1002/2017GL076085.